Preparation of nonaggregated silver nanoparticles by the liquid phase plasma reduction method

Heon Lee, Sung Hoon Park, and Sang-Chul Jung[a)]
Department of Environmental Engineering, Sunchon National University, Sunchon, Jeonnam 540-742, Republic of Korea

Je-Jung Yun
Nano Bio Research Center, Jangseong, Jeonnam 515-893, Republic of Korea

Sun-Jae Kim
Faculty of Nanotechnology and Advanced Materials Engineering, Sejong University, Seoul 143-747, Republic of Korea

Do-Heyoung Kim
School of Applied Chemical Engineering and Research Institute for Catalysis, Chonnam National University, Gwangju 500-757, Republic of Korea

(Received 6 November 2012; accepted 22 February 2013)

The liquid phase plasma reduction method has been applied to prepare silver nanoparticles from a solution of silver nitrate ($AgNO_3$) using a bipolar pulsed electrical discharge system. The excited states of atomic silver, hydrogen and oxygen as well as the molecular bands of hydroxyl radicals were detected in the emission spectra. As the discharge duration increased up to 10 min, silver particle peaks produced by surface plasmon absorption were observed around 430 nm. Both the particle size and the particle numbers were observed to increase with the length of the plasma treatment time and with the initial $AgNO_3$ concentration. Spherical nanoparticles of about 5–20 nm in size were obtained with the discharging time of 5 min, whereas aggregates of nanoparticles of about 10–50 nm in size were mainly produced with the discharging time of 20 min. The cationic surfactant of cetyltrimethylammonium bromide (CTAB) added with the CTAB/$AgNO_3$ molar ratio of 30% was shown to inhibit nanoparticle aggregation.

I. INTRODUCTION

Nanotechnology is a rapidly developing field, attracting significant investment from government, industry, and academia. Metal nanoparticles have gained much attention in recent years due to their notable properties, which are quite different from those of bulk substances, for potential applications in optical and electronic devices.[1–5] Among the wide variety of metal nanoparticles, considerable efforts have been devoted to the controlled synthesis and investigation of silver metal (Ag) nanoparticles.[6–8] Because of their optical, electrical and chemical properties, there is high interest in the potential applications, such as quantum dots, miniaturized electronic devices and catalysts for organic reactions.[9–11] Many are now actively involved in the synthesis of these metal nanoparticles, and a variety of preparation methods can be found in the literature, such as radiation chemical reduction,[12,13] chemical reduction in an aqueous medium with or without stabilizing polymers,[14,15] chemical or photoreduction in reverse micelles,[16,17] liquid-phase plasma method,[18–20] etc. Liquid-phase plasma (LPP) has attracted much attention, because it is a simple and practicable method, and the size distribution, morphology, and composition of nanoparticles can be controlled easily. Metal ions can be reduced to zero-valent metal if sufficient amount of electrons are provided. In LPP, large quantity of electrons are produced, which facilitate the reduction of metal ions to metal precipitates in liquid, forming nanoparticle suspension.

In this study, the LPP reduction method was applied to prepare silver nanoparticles from a solution of silver nitrate ($AgNO_3$), using a bipolar pulsed electrical discharge system. The affecting factors were investigated, including the $AgNO_3$ concentration, surfactant concentration, discharge duration and the morphology of the resultant particles. The features of nanocrystals have been characterized using transmission electron microscopy (TEM).

II. EXPERIMENTAL METHODS

The LPP experimental device (Fig. 1) consists of four main parts: (i) an LPP reduction reactor with two tungsten electrodes, (ii) a power supply system which can control the pulsed discharge parameters, (iii) a reactant solution for cooling and circulation, and (iv) a spectroscopic analysis system for the detection of optical emission spectra.

[a)]Address all correspondence to this author.
e-mail: jsc@sunchon.ac.kr
DOI: 10.1557/jmr.2013.59

 © Materials Research Society 2013

https://doi.org/10.1557/jmr.2013.59 Published online by Cambridge University Press

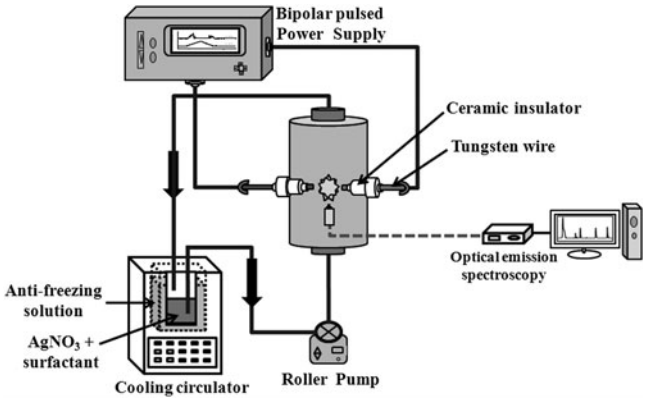


FIG. 1. Schematic of the liquid phase plasma experimental device for synthesis of silver nanoparticles.

The pulsed electric discharge was generated by a needle-to-needle electrode geometry system in an annular tube reactor (outer diameter 40 mm, height 80 mm). Tungsten electrodes (~diameter: 2 mm, 99.95% purity, T T M Korea Co., Paju, Gyeonggi-Do, Republic of Korea) with a ceramic insulator coating were used with an interelectrode gap of 0.2 mm. A high-frequency bipolar pulse power supply (Nano technology lnc., NTI-500W, Daejeon, Republic of Korea) was utilized to generate pulsed electrical plasma discharge directly in liquid phase. The bipolar pulse system is used for symmetrical plasma generation and immediate cleaning of the tip of both electrodes of any possible products adjacent to either cathode or anode, thus ensuring stable operating conditions. The reactant solutions were thermally equilibrated in a cold-water bath at 298 K and then circulated into the reactor using a roller pump. Spectroscopic measurements were performed during the electrical discharges for the tungsten electrodes using an AvaSpec-3648 Fiber optical spectrometer (Avantes Inc., Broomfield, CO).

Figure 2 shows a photograph of the LPP reactor used in this study with the plasma on. A strong glare was shown between the tungsten electrodes. The application of low voltage to the LPP system generated only bubbles between the electrodes, whereas increasing the voltage eventually (at 200 V) led to the generation of plasma between the electrodes resulting from breakdown. LPP exhibits a variety of properties upon the application of an external voltage, such as breakdown, overcurrent, photon emission, heat release, and vibration. The dielectric breakdown of liquid is explained by the breakdown theory of gas. Electrons accelerated by an applied electric field collide with liquid molecules, causing them to be ionized. Silver nitrate ($AgNO_3$; Junsei Chemicals Co. Ltd., Tokyo, Japan) was used to prepare 300 mL solutions with $AgNO_3$ concentrations of 2 mM. The electrical conductivity of the reactant solution prepared was 800 μS/cm.

To prevent aggregation among the Ag nanoparticles, cetyltrimethylammonium bromide [CTAB; $CH_3(CH_2)_{15}N(CH_3)_3Br$] was used as a surfactant. The addition of surfactant is known to affect the nanoparticle generation process due to the electrostatic interaction between the nanoparticle surface and the surfactant. It was reported in a previous study that the size, morphology, and degree of dispersion in the solution of ZnO particles were changed by the presence of surfactant.[21] Surfactant molecules composed of hydrophilic part and hydrophobic part effectively surround the nanoparticles produced, repel silver ions diffusing toward the particles, and isolate the particles to prevent aggregation between them. The water used in this work was ultrapure water (Daejung Chemicals & Metals Co., Ltd., Shiheung, Gyeonggi-Do, Republic of Korea). The obtained silver nanoparticles were observed by transmission electron microscopy (TEM; FEI make, model No. Tecnai20, Hillsboro, OR).



FIG. 2. Photograph of liquid phase plasma reactor and tungsten electrodes.

III. RESULTS

Optical emission spectra measurements were used to obtain information about the excited species in the discharge. The optical emission spectra acquired during the discharge with (i) ultrapure water and (ii) 2 mM $AgNO_3$ aqueous solution are shown in Fig. 3. The emission was detected with an optical fiber extending perpendicularly from the axis of the electrodes. The experimental conditions were kept constant during the spectra acquisition (discharge voltage 250 V, frequency 30 kHz, and pulse width 2 μs). It was possible to generate plasma using the power supply used in this study only within the frequency range of 25–30 kHz under the conditions of discharge voltage 250 V and the pulse width 2 μs. The plasma intensity was highest when the frequency was 30 kHz.

https://doi.org/10.1557/jmr.2013.59 Published online by Cambridge University Press

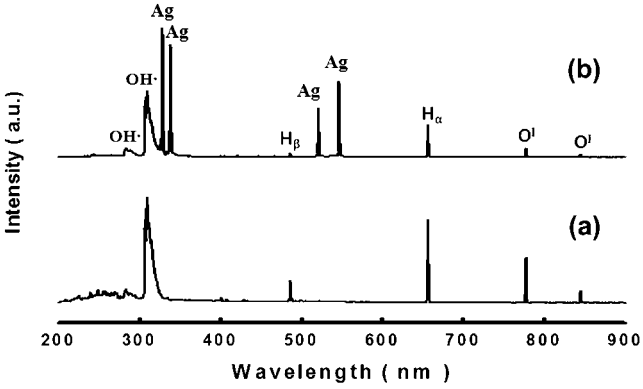


FIG. 3. Spatially and temporally integrated emission spectra for the discharge with (a) ultrapure water and (b) 2 mM $AgNO_3$ aqueous solution.

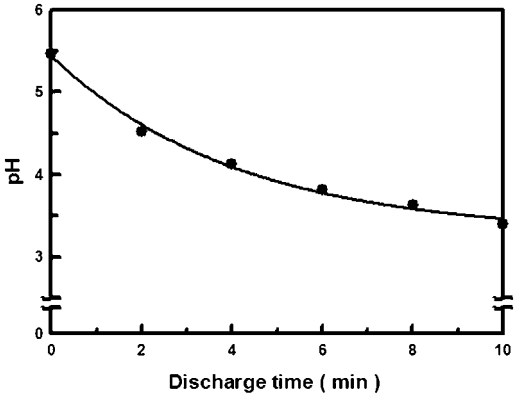


FIG. 4. Change in the aqueous solution pH as a function of discharge duration.

When the experiment was performed at 25 kHz, the amount of particles produced was much less because the plasma generation was less vigorous, but the particles generated were similar in size. Therefore, only the results obtained with the frequency of 30 kHz are presented in this article. We identified the chemical species produced by the discharge using optical emission spectroscopy. The excited states of atomic silver (at 328.2, 338.4, 520.9, and 546.6 nm), atomic hydrogen (at 656.3 and 486.1 nm) and atomic oxygen (at 777 and 844 nm) were detected in the emission spectra, as well as the molecular bands of the hydroxyl radical OH (at 283 and 309 nm). Silver nanoparticles were prepared by reaction with hydrogen radicals from the $[AgNO_3]^-$ ion aqueous solution, which was found through optical emission spectra analysis. LPP provides extremely rapid reactions caused by activated chemical species and radicals under high pressure. Liquid-phase chemical reduction methods for the synthesis of metal particles have been reported.[22,23]

Figure 4 shows the change in the $AgNO_3$ aqueous solution pH as a function of discharge duration. The initial $AgNO_3$ concentration was 2 mM. The amount of CTAB added was 30% (the surfactant/$AgNO_3$ molar ratio %). It is shown in Fig. 5 that the solution pH steadily decreased during the treatment. The optical emission spectra (Fig. 3) showed that atomic hydrogen, atomic oxygen, and hydroxyl radical OH were generated by the LPP. It is believed that the oxygen radicals reacted with molecular nitrogen (N_2) dissolved in the solution to produce nitric acid (HNO_3), which contributed to the decrease in pH. The OH radicals produce hydrogen peroxide (H_2O_2), and the hydrogen radicals are used for the reduction process to generate Ag nanoparticles. The role of hydrogen radicals in the synthesis of metal nanoparticles in solution plasma has been suggested based on electron spin resonance spectroscopic (ESR) measurements.[19] Metal particles are generally classified as hydrophobic colloids, and the charge on their surface, which is usually negative, is determined by the pH of the solution and their concentration. Ag particles exhibit strong repulsive force due to the negative surface charge, inhibiting particle aggregation. For overcoming this phenomenon, efforts have been made to control the pH, or to lower the zeta potential by combining opposite charges. The surface charge of metal nanoparticles is determined by the condition of the solution. The negative surface charge induces repulsive force among the particles, preventing the particles from coagulating.

Figure 5 shows ultraviolet-visible (UV–Vis) spectra of the plasma-treated $AgNO_3$ aqueous solutions obtained with different discharge durations. The plasma treatment was conducted with a discharge voltage of 250 V, frequency of 30 kHz, and pulse width of 2 μs. A 2-mM $AgNO_3$ solution (electrical conductivity 800 μS/cm) containing 30% CTAB was used. As the discharge duration increased, silver particle peaks produced by surface plasmon absorption were observed around 430 nm. This absorption peak at around 430 nm broadens due to nonuniformity of the silver crystallite size. The UV-Vis spectra for the Ag particles generated with different surfactant doses (10–50%) were all very similar (not shown) because the peak shape of UV-Vis spectra is determined not by the "polydispersity" of aggregate particle size but by the "polydispersity" of silver crystallite size, which is not affected by the presence of the surfactant. (Surfactant suppresses the aggregation between the primary nanoparticles, preventing the formation of aggregate particles).

Figure 6 shows TEM images of silver nanoparticles obtained with different discharge durations. Four different initial $AgNO_3$ concentrations were used: 2 mM (800 μS/cm), 10 mM (1,241 μS/cm), 25 mM (1,713 μS/cm), and 50 mM (5,720 μS/cm). At 50 mM (5,720 μS/cm), plasma was not generated because the electrical conductivity was too high. The plasma treatment conditions were the same as in Fig. 5. Surfactant was not used at this stage. Spherical nanoparticles of about 5–20 nm size were observed in the solution after 5 min. Also, spherical, dendrite-shaped nanoparticles were

https://doi.org/10.1557/jmr.2013.59 Published online by Cambridge University Press

mainly observed in the solution after 10 min. However, the size and amount of the nanoparticles in the solution increased compared to a discharge running for 5 min. After 20 min, spherical, dendrite-shaped nanoparticles of about 10–50 nm in size were mainly produced. Both the particle size and the particle number were observed to increase with the length of plasma treatment time. The number of nanoparticles generated increased with increasing initial $AgNO_3$ concentration. The nanoparticle size also increased with increasing initial $AgNO_3$ concentration especially at large plasma treatment duration (20 min).

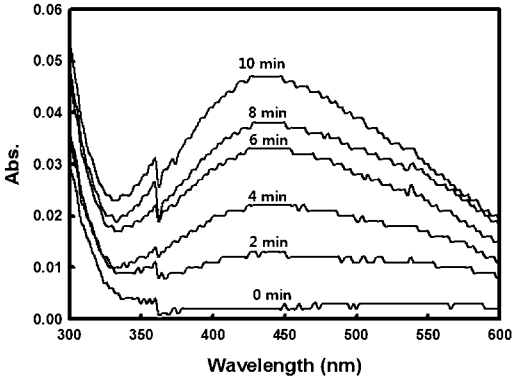


FIG. 5. UV–Vis spectra of plasma-treated $AgNO_3$ aqueous solution with varying discharge durations.

Silver nanoparticles with rounded-shape phase were observed by high-resolution TEM. The distance measured between the adjacent lattice fringes was about 2.25 Å. The electron diffraction pattern indicated that the silver nanoparticles generated in this study had polycrystalline structure. An energy-dispersive x-ray (EDX) spectrum of the same silver nanoparticle sample demonstrated the distinct presence of silver peaks. Bromium (Br) peaks could also be seen due to the presence of the CTAB used to prevent coagulation between the Ag nanoparticles. Peaks for tungsten (W), which was used for the electrodes, were also observed. The composition of the Ag nanoparticles was 96.18% (Ag), 2.49% (Br), and 1.34% (W).

The effects of the addition of surfactants on the particle size, the particle shape, and the dispersion of the silver nanoparticles generated in the LPP system were

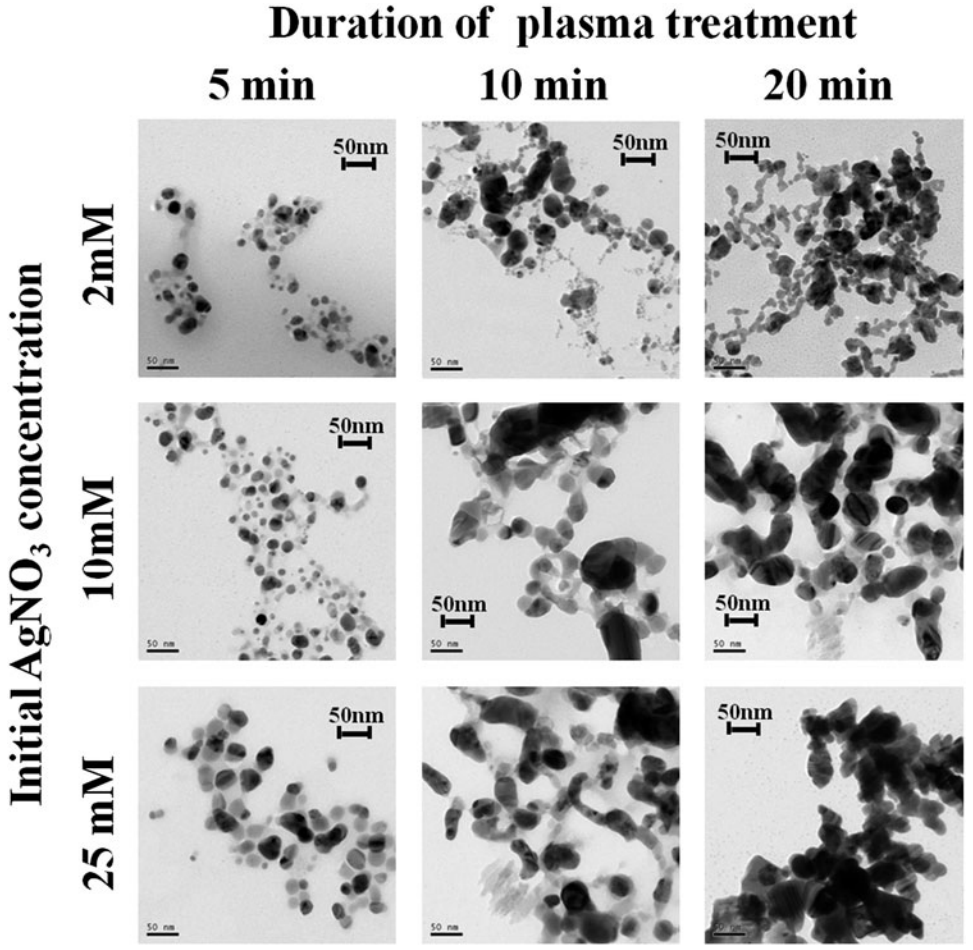


FIG. 6. TEM images of Ag nanoparticles synthesized using LPP reduction in aqueous solution with different discharge durations and initial $AgNO_3$ concentrations. All the scale bars denote 50 nm.

https://doi.org/10.1557/jmr.2013.59 Published online by Cambridge University Press

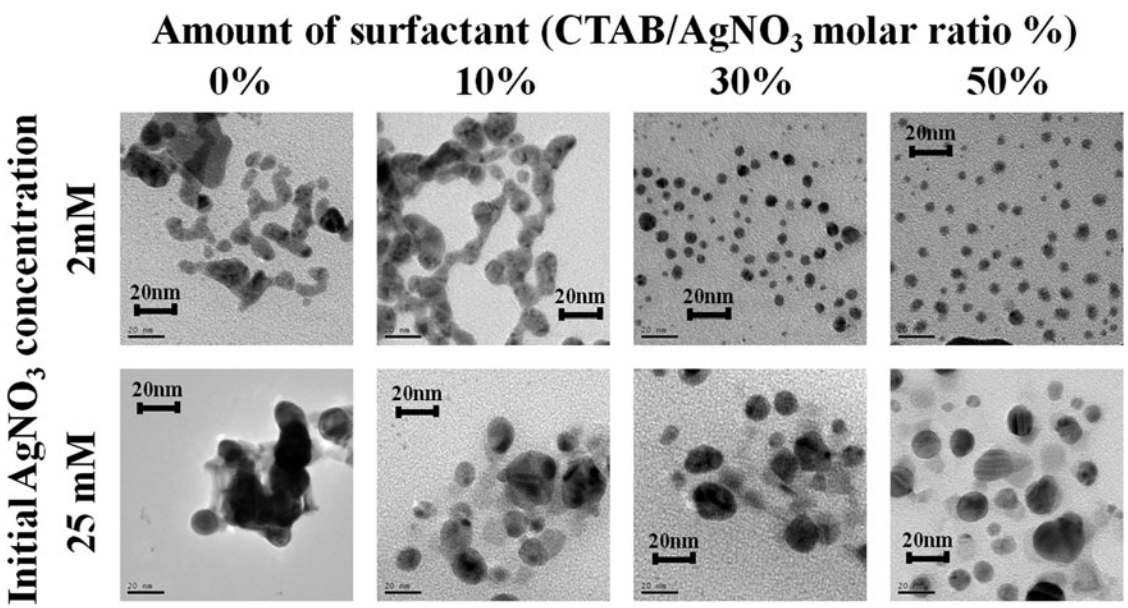


FIG. 7. TEM images of Ag nanoparticles synthesized using LPP reduction process with 20-min plasma duration in aqueous solution with different CTAB doses and initial $AgNO_3$ concentrations. All the scale bars denote 20 nm.

investigated. Figure 7 shows the TEM images of the silver nanoparticles generated by adding 0–50% CTAB with two different initial $AgNO_3$ concentrations: 2 mM (800 μS/cm) and 50 mM (5,720 μS/cm). For all the experiments described in this study, the plasma treatment duration was 20 min. The effect of CTAB on the Ag particle size and polydispersity was 2-fold. First, the growth of the (primary) Ag nanoparticles was suppressed by CTAB because it repelled Ag ions diffusing toward the particles. However, the polydispersity of the primary particles was not affected much by this effect as was indicated by UV–Vis spectra of plasma. Meanwhile, aggregation between the primary particles was inhibited by CTAB, resulting in suppression of particle growth by aggregation. The polydispersity of (both nonaggregated and aggregated) Ag particles was, therefore, greatly reduced by this effect. When 10% CTAB was added, tangled silver nanoparticles were still observed, similar to the dendrite-shaped silver nanoparticles generated without the addition of CTAB. However, the particle size generally became smaller after the addition of 10% CTAB. This trend continued when 20% CTAB was added (not shown). When the amount of CTAB added was 30%, on the other hand, spherical silver nanoparticles were mainly observed. When the amount of CTAB added was 20% or less, the particles were aggregated with a very low degree of dispersion. But when the amount of CTAB added was 30% or more, smaller silver nanoparticles were well dispersed in the solution. Again, as in Fig. 6, the nanoparticle size increased with increasing initial $AgNO_3$ concentration. A surfactant molecule is composed of a hydrophilic part with electrical charge, and a nonpolar hydrophobic part. When the cationic surfactant CTAB is used, the positive hydrophilic part of CTAB is oriented toward the surface of the negative silver particle surface, covering the silver particles effectively and repelling silver ions. This effect of CTAB is believed to have led to the generation of small nanoparticles.

IV. CONCLUSION

To use the LPP system for synthesis of silver nanoparticles, a series of experiments were performed, and the effects of LPP was evaluated. The conclusions obtained from the experimental results are as follows:

(1) The excited states of atomic silver, hydrogen and oxygen as well as the molecular bands of the hydroxyl radical OH were detected in the emission spectra for the discharge using tungsten needle electrodes.

(2) As the discharge duration increased, silver particle peaks produced by surface plasmon absorption were observed around 430 nm.

(3) Both the silver particle size and the silver particle numbers were observed to increase with the duration of plasma treatment and with the initial $AgNO_3$ concentration.

(4) When the amount of CTAB added was 20% or less, the particles were aggregated. But when the amount of CTAB added was 30% or more, the smaller silver nanoparticles were well dispersed in the solution.

(5) The composition of nanoparticles generated was 96.18% (Ag), 2.49% (Br), and 1.34% (W).

ACKNOWLEDGMENTS

This research was financially supported by the Ministry of Knowledge Economy (MKE), Korea Institute for Advancement of Technology (KIAT) through the Inter-ER Cooperation Projects.

https://doi.org/10.1557/jmr.2013.59 Published online by Cambridge University Press

REFERENCES

1. L. Balan and D. Burget: Synthesis of metal/polymer nanocomposite by UV-radiation curing. *Eur. Polym. J.* **42**, 3180 (2006).
2. I.O. Sosa, C. Nognez, and R.G. Barrera: Optical properties of metal nanoparticles with arbitrary shapes. *J. Phys. Chem. B.* **107**, 6269 (2003).
3. T. Hayashi, T. Ohno, S. Yatsuya, and R. Uyeda: Formation of ultrafine metal particles by gas-evaporation technique. *J. Appl. Phys.* **16**, 705 (1976).
4. P. Barnickel and A. Wokaun: Synthesis of metal colloids in inverse microemulsions. *Mol. Phys.* **69**, 1 (1990).
5. Y. Sun and Y. Xia: Gold and silver nanoparticles: A class of chromophores with colors tunable in the range from 400 to 750 nm. *Analyst* **128**, 686 (2003).
6. P. Barnickel and A. Wokaun: Silver coated latex spheres. Optical absorption spectra surface enhanced Raman scattering. *Mol. Phys.* **57**, 1355 (1989).
7. H.Q. Jiang, S. Manolache, A.C.L. Wong, and F.S. Denes: Plasma-enhanced deposition of silver nanoparticles onto polymer and metal surfaces for the generation of antimicrobial characteristics. *J. Appl. Polym. Sci.* **93**, 1411 (2004).
8. J. Xu, X. Han, H. Lin, and Y. Hu: Synthesis and optical properties of silver nanoparticles stabilized by gemini surfactant. *Colloids Surf., A* **273**, 179 (2006).
9. W. Cai, Y. Zhang, J. Jia, and L. Zhang: Semiconducting optical properties of silver/silica mesoporous composite. *Appl. Phys. Lett.* **73**, 2709 (1998).
10. A.K. Pal, S. Hussain, and R.K. Roy: Incorporation of silver nanoparticles in DLC matrix and surface plasmon resonance effect. *Chem. Phys.* **99**, 375 (2006).
11. J.J. Mock, M. Barbic, and D.R. Smith: Silver nanodisks: Synthesis, characterization, and self-assembly. *J. Chem. Phys.* **116**, 6755 (2002).
12. J.P. Abid, A.W. Wark, P.F. Brevet, and H. Girault: Preparation of silver nanoparticles in solution from a silver salt by laser irradiation. *Chem. Commun.* **7**, 92 (1993).
13. K. Zou, X.H. Zhang, X.F. Duan, X.M. Meng, and S.K. Wu: Seed-mediated synthesis of silver nanostructures and polymer/silver nanocables by UV irradiation. *J. Cryst. Growth* **273**, 285 (2004).
14. A. Pal, S. Shah, and S. Devi: Synthesis of Au, AgAu–Ag alloy nanoparticles in aqueous polymer solution. *Colloids Surf., A* **302**, 51 (2007).
15. Y. Xiong, A.R. Siekkinen, J. Wang, Y. Yin, M.J. Kim, and Y. Xia: Synthesis of silver nanoplates at high yields by slowing down the polyol reduction of silver nitrate with polyacrylamide. *J. Mater. Chem.* **17**, 2600 (2007).
16. M.M. Oliveira, D. Ugarte, D. Zanchet, and A. Zarbin: Influence of synthetic parameters on the size, structure and stability of dodecanethiol-stabilized silver nanoparticles. *J. Colloid Interface Sci.* **292**, 429 (2005).
17. W. Zhang, X. Qiao, and J. Chen: Synthesis of nanosilver colloidal particles in water/oil microemulsion. *Colloids Surf., A* **299**, 22 (2007).
18. J.K. Lung, J.C. Huang, D.C. Tien, C.Y. Liao, K.H. Tseng, T.T. Tsung, W.S. Kao, T.H. Tsai, C.S. Jwo, H.M. Lin, and L. Stobinski: Preparation of gold nanoparticles by arc discharge in water. *J. Alloys Compd.* **434**, 655 (2007).
19. N. Saito, J. Hieda, and O. Takai: Synthesis process of gold nanoparticles in solution plasma. *Thin Solid Films* **518**, 912 (2009).
20. C. Richmonds and R.M. Sankaran: Plasma-liquid electrochemistry: Rapid synthesis of colloidal metal nanoparticles by microplasma reduction of aqueous cations. *Appl. Phys. Lett.* **93**, 131501 (2008).
21. Y. Chung and W. Kang: Preparation of ZnO nanoparticles by laser ablation of dispersed ZnO powder in solution. *J. Korean Chem. Soc.* **50**, 440 (2006).
22. Š. Potocký, N. Saito, and O. Takai: Needle electrode erosion in water plasma discharge. *Thin Solid Films* **518**, 918 (2009).
23. P. Baroch, V. Anita, N. Saito, and O. Takai: Bipolar pulsed electrical discharge for decomposition of organic compounds in water. *J. Electrostatics* **66**, 294 (2008).

https://doi.org/10.1557/jmr.2013.59 Published online by Cambridge University Press